Eur. Phys. J. B **25**, 263–268 (2002)
DOI: 10.1140/epjb/e20020030

**THE EUROPEAN PHYSICAL JOURNAL B**
EDP Sciences


# Ordering of the vortex lattice in Mo-Re films

T. Di Luccio[1], C. Attanasio[1], A. Andreone[2], and A.M. Cucolo[1,a]

[1] Dipartimento di Fisica "E.R. Caianiello" and Unità INFM, Università degli Studi di Salerno, Baronissi (Sa), 84081, Italy
[2] Dipartimento di Scienze Fisiche and Unità INFM, Università degli Studi di Napoli "Federico II", Napoli, 80125, Italy

Received 20 July 2001

**Abstract.** We investigated the vortex lattice ordering induced by an applied current in thick (700–900 nm) Mo-Re films with strong pinning. Measurements of $I$-$V$ characteristics as a function of field and at different temperatures were carried out. We found that, as in the case of weakly pinning amorphous samples, dynamic ordering can occur only if the size of the vortex correlated region is at least two times the intervortex distance.

**PACS.** 74.60.Ge Flux pinning, flux creep, and flux-line lattice dynamics – 74.60.Jg Critical currents – 74.76.Db Conventional superconducting films

## 1 Introduction

It is well known that ordering of the vortex lattice can be induced by an external current in a superconductor with the presence of pinning. This fact, early observed in neutron diffraction experiment [1], has recently gained a renewed attention, and a lot of theoretical [2–4], numerical [5–8] and experimental [9,10] studies have been performed on this subject. Several interesting phenomena have been predicted about the dynamic phase transitions of the vortex lattice, depending on the competition between the pinning strength due to a random distribution of material defects and the intervortex interactions. In particular, it has been established that, increasing the applied current, a pinned vortex lattice first flows plastically and then elastically, forming an ordered lattice [11]. One of the fingerprints of the vortex lattice dynamic transition is the change of slope in the $I$-$V$ characteristics which is reflected in the appearance of a peak in the $\mathrm{d}V/\mathrm{d}I$ *versus* $I$ curves [12]. This effect has been reported for amorphous MoGe [13,14] and NbGe [15] thin films and indicated as *dynamic ordering*. In both cases the samples were characterized by moderate pinning and relatively low values of the critical current density $J_c$. For this reason the increase of the rigidity of the moving vortex configuration has been interpreted in terms of the two dimensional (2D) collective pinning theory by Larkin and Ovchinnikov [16].

In this paper we report on $I$-$V$ measurements carried out on several Mo-Re films of different stoichiometry. With respect to the previous experiments [13–15] our samples are characterized by higher $J_c$ values and they could be analyzed in the framework of the three dimensional (3D) collective pinning [16]. Among all the measured samples a clear peak in the dynamic resistance *versus* $I$ curves has been observed in a definite part of the $B$-$T$ plane only for one sample, for which $R_c$, the size of the correlated regions in the direction perpendicular to the field direction, is at least two times the intervortex distance, $a_0$.

[a] e-mail: cucolo@sa.infn.it

## 2 Experimental

Mo-Re films of two different compositions (in particular $Mo_{60}Re_{40}$ and $Mo_{75}Re_{25}$, as determined by Electron Dispersive Spectroscopy (EDS) analysis) were prepared by sputtering onto heated sapphire substrates [18,19]. Mo-Re is considered as an "atypical" A-15 compound since its maximum transition temperature is associated to out-of-stoichiometry compositions [20]. This feature seems to indicate that the correlation between $T_c$ and the long range order in the (Mo) chains is less pronounced and therefore less sensitive to structural disorder than in other A-15 superconductors. Moreover, even when the material is grown in amorphous phase, it shows quite large values of the critical temperature and critical current. Base pressure in the deposition chamber was in the $10^{-8}$ torr range, with approximately $1.0 \times 10^{-3}$ torr Ar as sputtering gas. Typical evaporation rates were around 5 nm/s and thicknesses $d$ of the films ranged from 700 to 900 nm. Rates and thicknesses were measured during the deposition by an oscillating quartz crystal monitor. Depending on the value of the substrate temperature $T_s$ during the deposition, samples of different crystal structures were obtained. In particular, all the samples we have deposited for this study at $T_s$ less than 600 °C were completely amorphous as proved by high-angle $\Theta$-$2\Theta$ X-ray diffraction patterns which do not show the presence of any peak related to

**Table 1.** Physical parameters for two of the measured samples. The stoichiometry of the sample MR6 (MR19) is Mo = 75 (60)% and Re = 25 (40)%. Both the samples are completely amorphous and do not show a clear A-15 structure, as proved by X-Ray diffraction measurements. See the text for the meaning of the listed quantities.

| Sample | $d$(nm) | $\rho_{10\ \mathrm{K}}$ ($\mu\Omega$ cm) | $\rho_{300\ \mathrm{K}}/\rho_{10\ \mathrm{K}}$ | $T_\mathrm{c}$ (K) | $S$(T/K) | $\xi(0)$ (nm) | $B_{c2}(0)$ (T) | $\kappa$ | $\lambda(0)$ (nm) |
|---|---|---|---|---|---|---|---|---|---|
| MR6 | 770 | 12 | 1.8 | 9.71 | 0.2 | 15 | 1.4 | 5.48 | 134 |
| MR19 | 720 | 57 | 1.2 | 10.71 | 0.25 | 13 | 1.84 | 13.36 | 283 |

the A-15 cubic structure. These samples have reduced superconducting critical temperature ($T_\mathrm{c} \approx 9 - 10$ K) and critical current density at low field and temperature ($J_\mathrm{c} \approx 10^8 - 10^9$ A/m$^2$) with respect to the samples deposited at higher temperatures. In this case the films have a clear A-15 structure, $T_\mathrm{c} \approx 13 - 15$ K and $J_\mathrm{c} \approx 10^{10}$ A/m$^2$ [18–20].

After the deposition the samples were patterned into strips having length $l = 1$ mm and width $w = 100\ \mu$m. The strips were obtained by a standard photolithographic technique followed by chemical etching. The superconducting critical temperature and the upper critical field $B_{c2}(T)$ were resistively measured and a superconducting Nb-Ti solenoid was used to produce the external magnetic field. The field was always applied perpendicular to the sample and to the direction of the flowing current. The $T_\mathrm{c}$ and $B_{c2}$ values were extracted from the $R(T)$ curves taking the 50% value of the normal state resistance $R_\mathrm{N}$ just above the transition to the superconducting state. The transition widths, estimated from the temperature difference at 10% and 90% of $R_\mathrm{N}$, were typically less than 20 mK at zero field for all the samples and did not appreciably broaden even in high magnetic field, confirming the high quality of our films. The applied dc bias current density was $\sim 10^6$ A/m$^2$, much lower than $J_\mathrm{c}$. The low temperature resistivity values $\rho_{10\ \mathrm{K}}$ were around 50 $\mu\Omega$ cm and 10 $\mu\Omega$ cm for the $Mo_{60}Re_{40}$ and the $Mo_{75}Re_{25}$ samples respectively. In the former case the ratio $\rho_{300\ \mathrm{K}}/\rho_{10K}$ is close to the unity, while for the latter it is always around 2. Finally the $J_\mathrm{c}$ values were obtained from the $I$-$V$ curves using the criterion described in the next section. Since $I$-$V$ curves were measured up to high current densities, in order to eliminate heating effects, samples were directly immersed in liquid helium. The dynamic resistance $R_\mathrm{d} = \mathrm{d}V/\mathrm{d}I$ was numerically calculated from the *dc* measurements using a standard computation algorithm. Occasionally $R_\mathrm{d}$ has been also directly measured and no differences were observed.

## 3 Results and discussion

In the following we report on $I$-$V$ characteristics performed on eight different Mo-Re films. In Table 1 are summarized all the relevant physical parameters characterizing the sample on which the in $R_\mathrm{d}$ has been observed, namely the sample MR6. The stoichiometry of this sample is Mo = 75% and Re = 25%. In Table 1 are also reported the same quantities for the sample MR19 representative of the samples on which no dynamic ordering has been observed. The stoichiometry of this sample is Mo = 60% and Re = 40%. The Ginzburg-Landau (GL) coherence length $\xi(0)$ is obtained from the slope $S$ of the upper critical magnetic field at $T_\mathrm{c}$, $S = -\mathrm{d}B_{c2}/\mathrm{d}T|_{T_\mathrm{c}}$, using the relation

$$B_{c2}(0) = 0.69 S T_\mathrm{c} = 0.69 \frac{\phi_0}{2\pi\xi(0)^2} \tag{1}$$

which is also used to determine the upper critical field at zero temperature [21]. For the sample MR6 the BCS coherence length $\xi_0$ is found to be 70 nm from the relation $\xi_0 = \hbar v_\mathrm{F}/\pi\Delta(0)$ where $v_\mathrm{F} = 5 \times 10^5$ m/s is the Fermi velocity [22] and $\Delta(0) = 1.8 k_\mathrm{B} T_\mathrm{c}$ [23] is the BCS superconducting gap at zero temperature. Finally the mean free path $\ell$ has been estimated to be 3 nm from the measured low temperature resistivity $\rho_{10\ \mathrm{K}}$ (expressed in $\mu\Omega$ cm), using the relation [24]

$$\ell = v_0 \left(\frac{0.22}{\rho_{10\ \mathrm{K}}}\right)\left(\frac{r_\mathrm{s}}{a}\right)^3 \times 10^{-14}\ \mathrm{s} \tag{2}$$

where $v_0$ is the average electronic velocity taken equal to $v_\mathrm{F}$ [24], $r_\mathrm{s}$ is a measure of the electronic density and $a$ is the Bohr radius. The $r_\mathrm{s}$ value has been deduced from the relation [24]

$$\gamma = (0.169) Z \left(\frac{r_\mathrm{s}}{a}\right)^2 \times 10^{-4}\ \mathrm{cal/mole\ K^2} \tag{3}$$

where $\gamma$ is the specific heat and $Z$ is the valence. Using the values $\gamma = 4$ mJ/mole K$^2$ and $Z = 6$ [25] we have obtained $r_\mathrm{s} = 0.156$ nm. Comparing the values of $\xi_0$ and $\ell$ it is clear that MR6 sample falls in the category of dirty type-II superconductors for which the Ginzburg-Landau parameter $\kappa$ has the expression $3.54 \times 10^4 \sqrt{\rho_{10\ \mathrm{K}} S}$ [26]. Finally if we estimate the value for $\xi_0$ from the relation $\xi(0) = 0.855(\xi_0 \ell)^{1/2}$, using the value of $\xi(0)$ extracted from Table 1, we get $\xi_0 \approx 100$ nm which, again, goes in the direction of $\xi_0 \gg \ell$. Similar results hold for all the measured samples.

Figure 1 shows the $I$-$V$ characteristics for the sample MR6 at $T = 3.1$ K for different applied magnetic fields in the range 0.05 T $< B <$ 1.2 T. Curves show a strong curved nature at low voltage and this makes the value of the critical current $I_\mathrm{c}$ strongly dependent on the voltage criterion chosen to determine it. For this reason, following the procedure already used in the case of NbGe thin

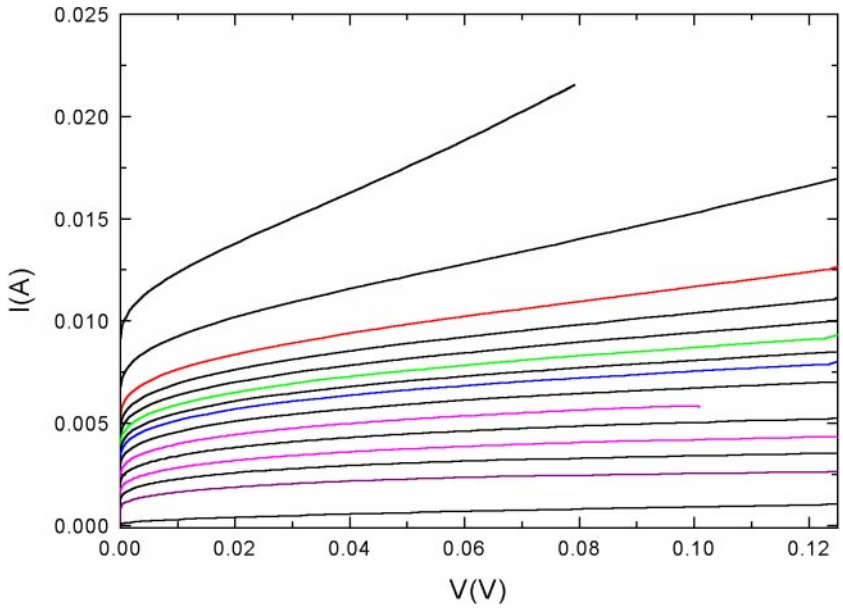


**Fig. 1.** *I-V* characteristics for the sample MR6 at $T = 3.1$ K for different applied magnetic fields. Curves correspond to increasing fields, from top to bottom, equal to 0.05, 0.1, 0.15, 0.2, 0.25, 0.3, 0.35, 0.4, 0.5, 0.6, 0.7, 0.8, 0.9, 1.0, 1.2 T.

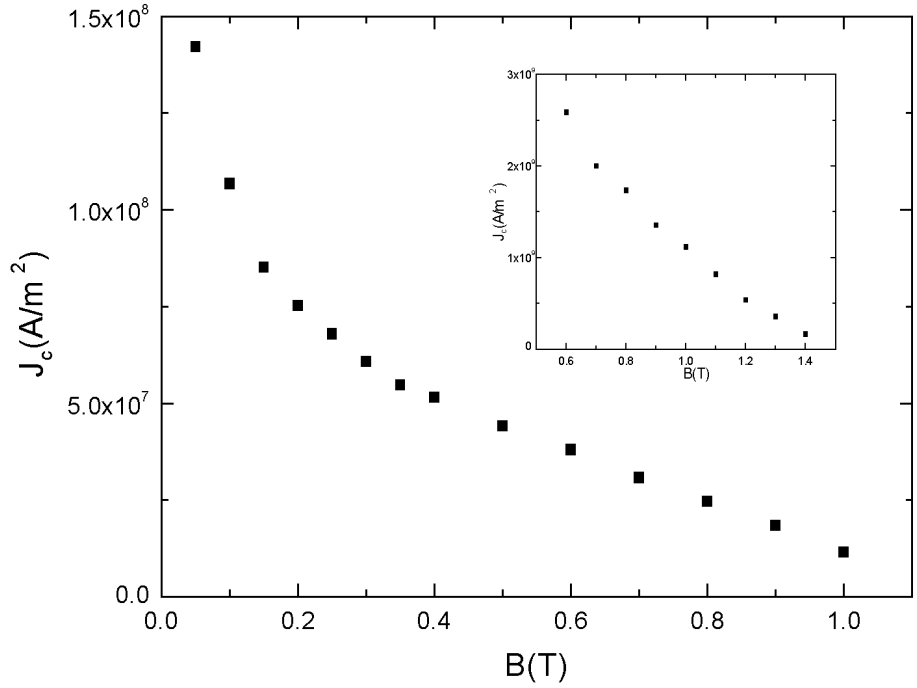


**Fig. 2.** $J_c$ *versus* applied magnetic field for the sample MR6 at $T = 3.1$ K ($t = 0.38$). Inset: Same as in the main panel for the sample MR19 at $T = 4.2$ K ($t = 0.39$).

films [15], $I_c$ has been determined by extrapolating the linear flux flow region (where the resistance $R_{ff}$ is equal to $\sim R_N B/B_{c2}$ [17]) down to $V = 0$. In our case the obtained full flux flow velocity at intermediate fields is $v \sim 35$ m/s and it is connected to the flux-flow voltage by the relation $V = vBl$, where $l$ is the length between the voltage probes. This value is larger than the values obtained for NbGe [15,27], consistently with the fact that we are dealing with samples with higher $J_c$. The critical current density *versus* the applied magnetic field for the sample MR6 at $T = 3.1$ K ($t \equiv T/T_c = 0.38$) is shown in Figure 2. The low field value of the critical current for the sample MR6, around $10^8$ A/m$^2$, is the lowest observed in all the other measured samples for comparable values of field and temperature. In the inset of Figure 2 the magnetic field dependence of $J_c$ for the sample MR19 at $T = 4.2$ K

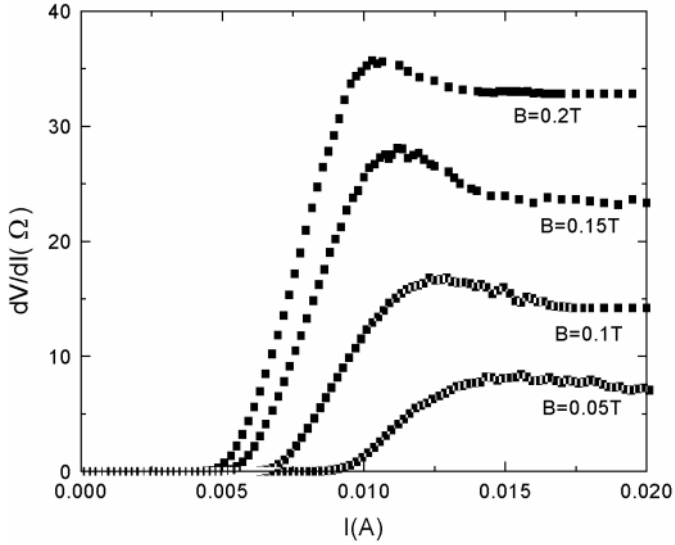


**Fig. 3.** Dynamic resistance $R_{\rm d}$ *versus* $I$ at $T = 3.1$ K for the sample MR6. The magnetic field values are 0.05, 0.1, 0.15, 0.2 T.

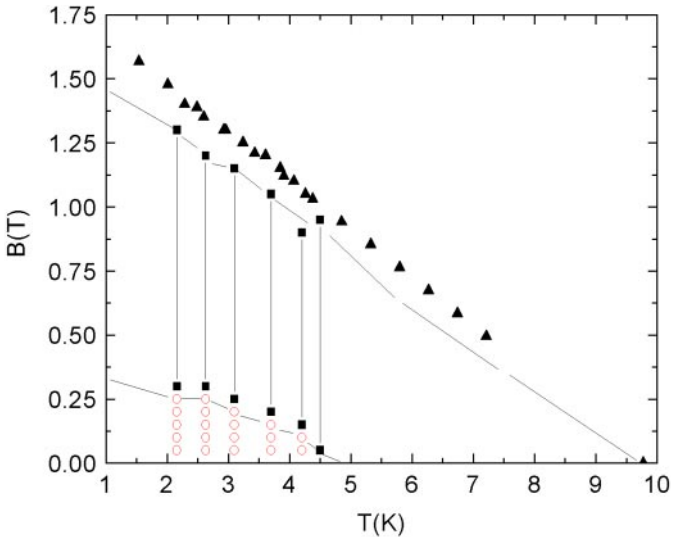


**Fig. 4.** $B$-$T$ phase diagram for the sample MR6. Up triangles are the measured $B_{c2}$ values, open circles are at fields and temperatures where dynamic ordering occurs and solid squares show the field interval where the peak in the $R_{\rm d}(I)$ was not observed. The smooth lines through the data points are a guide to the eye for the boundaries of the above different phases.

($t = 0.39$) is shown. At $B = 0.6$ T it is $J_{\rm c} \approx 3 \times 10^9$ A/m$^2$. Figure 3 shows the presence of a peak in the dynamic resistance $R_{\rm d}$ *versus* $I$ for different fields at $T = 3.1$ K for the sample MR6. No such peaks have been detected in all the other samples. For currents larger than the current at which the peak occurs, the dynamic resistance becomes equal to $R_{\rm ff}$. For the sample MR6 the $B$-$T$ phase diagram has been built and it is shown in Figure 4. Up triangles indicate the measured $B_{c2}$ values, the open circles represent the fields and temperatures where dynamic ordering occurs (because of the presence of a peak in the d$V$/d$I$ *versus* $I$ curves [12]) and solid squares delimit the field interval where, at a certain temperature, the peak in the $R_{\rm d}(I)$ was not observed anymore. Finally, using the expression for the melting transition temperature of a 3D vortex lattice $T_{\rm m}^{3D}$ [28], the melting curve is found to lie very close to the $B_{c2}$ line. This fact is also experimentally confirmed if the resistive transition curves are plotted in the Arrhenius fashion. In this case no clear change in the slopes of the curves has been observed, even at very low voltages, indicating that the mechanism of the vortex dynamics remains the same [29].

In order to give an interpretation of the increase of the ordering in the vortex lattice we use the 3D collective pinning theory [16]. According to this approach, a short range is preserved in the vortex lattice only inside a correlated volume $V_{\rm c}$ with length $L_{\rm c}$ along the field and with diameter $R_{\rm c}$ perpendicular to the field direction. $R_{\rm c}$ has the following expression [30]

$$R_{\rm c} = \sqrt{\frac{c_{66}\xi}{F_{\rm p}}} \tag{4}$$

where $F_{\rm p} = J_{\rm c}B$ is the measured pinning force density and the shear modulus $c_{66}$ is given by [31]

$$c_{66} = \frac{\phi_0 B}{16\pi\mu_0\lambda^2(T)}(1 - 0.29b)(1 - b)^2 \tag{5}$$

where $b = B/B_{c2}$ is the reduced magnetic field and $\lambda(T)$ is the temperature dependent penetration depth which, in our case is given by [26] $\lambda(T) = 1.63\kappa\xi(T)$.

Figure 5 shows values of the ratio $R_{\rm c}/a_0$ as a function of field for the sample MR6 at $T = 3.1$ K ($t = 0.38$). $R_{\rm c}$ is calculated from the measured $F_{\rm p}$ and using the expression (5). $a_0$ is field dependent according to the expression $1.075\sqrt{\phi_0/B}$. The values used in equations (4) and (5) for $\xi(T)$ (or $\lambda(T)$) are calculated from the zero temperature values using the expression $\xi(T) = \xi(0)/\sqrt{1 - T/T_{\rm c}}$ (or $\lambda(T) = \lambda(0)/\sqrt{1 - T/T_{\rm c}}$). The application of the 3D collective pinning theory to our samples is justified by the fact that the correlation length $L_{\rm c}$ is always smaller than the sample thickness. In fact, at $B = 0.5$ T $R_{\rm c}$ is $\approx 3.5a_0 \approx 250$ nm, and using the relation valid for large values of $\kappa$ and $\lambda$ and for $b < 0.5$ [32]

$$L_{\rm c} \approx 3\Big[b/(1 - b)\Big]^{1/2} R_{\rm c} \tag{6}$$

we find $L_{\rm c} = 539$ nm $\lesssim d$.

We observe that the calculated values of $R_{\rm c}/a_0$ are at low fields equal to 2 and never greater than 4. These values for $R_{\rm c}/a_0$ for the sample MR6 turn out to be much smaller than those reported for weakly pinning amorphous NbGe thin films [15]. This is in agreement with the assumption that strong disorder is present in our samples. In fact, evaluation of the ratio $R_{\rm c}/a_0$ for all the other measured

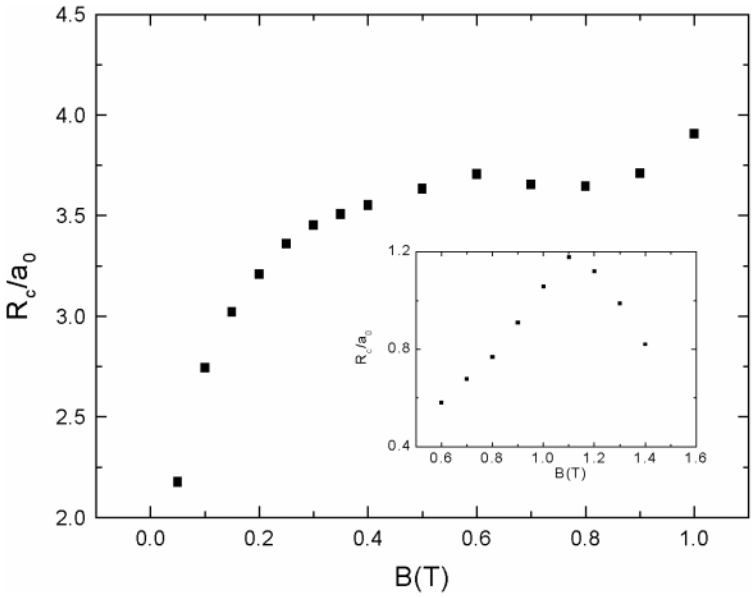


**Fig. 5.** $R_c/a_0$ *versus* $B$ for the sample MR6 at $T = 3.1$ K ($t = 0.38$). Inset: Same as in the main panel for the sample MR19 at $T = 4.2$ K ($t = 0.39$).

Mo-Re films gives values that are always of the order of the unit because of the higher values of the measured critical current (see the inset of Figure 5 where $R_c/a_0$ *versus* $B$ at $T = 4.2$ K ($t = 0.39$) for the sample MR19 is plotted). This could explain why we do not observe any ordering of the vortex lattice under the influence of the driving current in the stronger pinning Mo-Re films which are characterized by single vortex pinning.

Finally the above results confirm the results previously obtained on 2D collective pinning samples [15]. In fact, also in case of strong disordered Mo-Re samples, dynamic ordering occurs at low fields due to the fact that, when the pinning force is high, the vortex lattice can be plastically deformed also for small applied fields. The peak in $R_d$ disappears when increasing the magnetic field and the temperature toward $T_c$ because it is too close, and then undistinguishable, to the much larger peak related to the normal state transition.

## 4 Conclusions

In conclusion, the occurrence of dynamic ordering has been investigated in Mo-Re films of different stoichiometry and structural disorder. The samples, even amorphous, are fairly strong pinning and the flux line lattice is three dimensional. Also, they all fall in the category of dirty type-II superconductors. We observe that, regardless of the composition of the samples, current induced ordering takes place only if $R_c \gtrsim 2a_0$. For samples with higher current density, for which $R_c \approx a_0$, ordering of the vortex lattice cannot be established by the applied current. This result confirms that $R_c/a_0$ is the relevant parameter one should consider when evaluating the degree of disorder in the vortex dynamics of a superconducting sample.

## References

1. P. Thorel, J. Phys. France **34**, 447 (1973).
2. T. Giamarchi, P. Le Doussal, Phys. Rev. Lett. **76**, 3408 (1996).
3. M.C. Faleski, M.C. Marchetti, A.A. Middleton, Phys. Rev. B **54**, 12427 (1996).
4. L. Balents, M.C. Marchetti, L. Radzihovsky, Phys. Rev. B **57**, 7705 (1998).
5. H.J. Jensen, A. Brass, A.J. Berlinsky, Phys. Rev. Lett. **60**, 1676 (1988).
6. N. Grønbech-Jensen, A.R. Bishop, D. Dominguez, Phys. Rev. Lett. **76**, 2985 (1996).
7. K. Moon, R.T. Scattelar, G.T. Zimanyi, Phys. Rev. Lett. **77**, 2778 (1996).
8. C.J. Olson, C. Reichhardt, F. Nori, Phys. Rev. Lett. **81**, 3757 (1998).
9. S. Bhattacharya, M.J. Higgins, Phys. Rev. Lett. **70**, 2617 (1993).
10. U. Yaron, P.L. Gammel, D.A. Huse, R.N. Kleiman, C.S. Oglesby, E. Bucher, B. Batlogg, D.J. Bishop, K. Mortensen, K. Clausen, C.A. Bolle, F. De La Cruz, Phys. Rev. Lett. **73**, 2748 (1994).
11. M.J. Higgins, S. Bhattacharya, Physica C **257**, 232 (1996).
12. A.E. Koshelev, V.M. Vinokur, Phys. Rev. Lett. **73**, 3580 (1994).
13. M.C. Hellerqvist, D. Hephron, W.R. White, M.R. Beasley, A. Kapitulnik, Phys. Rev. Lett. **76**, 4022 (1996).
14. M.C. Hellerqvist, A. Kapitulnik, Phys. Rev. B **56**, 5521 (1997).
15. J.M.E. Geers, C. Attanasio, M.B.S. Hesselberth, J. Aarts, P.H. Kes, Phys. Rev. B **63**, 094511 (2001).
16. A.I. Larkin, Yu.N. Ovchinnikov, J. Low Temp. Phys. **34**, 409 (1979).
17. A.I. Larkin, Yu.N. Ovchinnikov, in *Nonequilibrium Superconductivity* (Elsevier Science Publishers, Amsterdam, 1986).

18. A. Andreone, A. Barone, A. Di Chiara, G. Mascolo, V. Palmieri, G. Peluso, U. Scotti di Uccio, IEEE Trans. Magn. **MAG-25**, 1972 (1989).
19. A. Andreone, A. Barone, A. Di Chiara, F. Fontana, G. Mascolo, V. Palmieri, G. Peluso, G. Pepe, U. Scotti di Uccio, J. Supercond. **2**, 493 (1989).
20. S.V. Vonsovsky, Yu.A. Izyumov, E.-Z. Kurmaev, *Superconductivity of Transition Metals* (Springer-Verlag, Berlin, 1982).
21. N.R. Werthamer, E. Helfand, P.C. Honenberg, Phys. Rev. **147**, 295 (1966).
22. M. Ashkin, D.W. Deis, M. Gottlieb, C.K. Jones, Physica **55**, 631 (1971).
23. J. Talvacchio, M.A. Janocko, J. Greggi, J. Low Temp. Phys. **64**, 396 (1986).
24. N.W. Ashcroft, N.D. Mermin, *Solid State Physics* (Saunders College, Philadelphia, 1976).
25. W.L. McMillan, Phys. Rev. **167**, 331 (1968).
26. P.H. Kes, C.C. Tsuei, Phys. Rev. B **28**, 5126 (1983).
27. P. Berghuis, P.H. Kes, Phys. Rev. B **47**, 262 (1993).
28. E.H. Brandt, Rep. Prog. Phys. **58**, 1465 (1995).
29. W.R. White, A. Kapitulnik, M.R. Beasley, Phys. Rev. Lett. **66**, 2826 (1991).
30. M. Tinkham, *Introduction to Superconductivity* (Mc Graw-Hill, Inc., 1996).
31. A. Pruymboom, P.H. Kes, Jpn J. Appl. Phys. **26-3**, 1533 (1987).
32. R. Wørdenweber, P.H. Kes, Phys. Rev. B **34**, 494 (1986).